Research articles

Spin-phonon coupling in hexagonal $Sr_{0.6}Ba_{0.4}MnO_3$

Ritu Rawat, D.M. Phase, R.J. Choudhary *

UGC DAE Consortium for Scientific Research, Indore 452001, M.P., India

ABSTRACT

We have probed the magnetic properties of hexagonal $Sr_{0.6}Ba_{0.4}MnO_3$ (SBMO) and its correlations with the vibrational spectra. Magnetization measurements reveal two antiferromagnetic transitions at 325 K and at 227 K. Temperature dependent Raman spectra of SBMO suggest that though structural symmetry is maintained across the transition temperatures, imprints of these magnetic transitions are noticed in anomalous behavior of Mn displacement E_{1g} mode position in the same temperature range. A_{1g} mode related to non-magnetic oxygen ion does not show such anomaly and follows an anharmonic behavior. Deviation from the anharmonic behavior of the E_{1g} mode and its absence in A_{1g} highlight the spin-phonon coupling in SBMO. The spin-phonon coupling parameter is evaluated to be $2.2 \, cm^{-1}$.

© 2017 Elsevier B.V. All rights reserved.

1. Introduction

AMnO₃ type manganites have been extensively studied over the last few decades since they exhibit wide range of exotic properties such as multiferroicity, colossal magneto-resistance, charge ordering, metal-insulator transition, etc., which have tremendous applications in several devices [1–4]. These properties emanate in such materials due to coupling among different degrees of freedom viz. charge, spin and lattice. Recently, it has been shown that strained film of cubic $SrMnO_3$ or its bulk sample doped with cation of different ionic radii displays strong spin-phonon coupling, which should be the driving force for induction of ferroelectricity in the material [5]. It has been shown by Goian et al. that such spin phonon coupling is observed in Ba doped cubic $SrMnO_3$, viz. $Sr_{0.6}Ba_{0.4}MnO_3$ [6]. $SrMnO_3$ is an antiferromagnetic insulator and can exist in cubic as well as hexagonal structure. When cubic $SrMnO_3$ is doped with Ba (having larger ionic radii than Sr^{2+}), it causes the displacement of Mn^{4+} ion and modulation in O–Mn–O bond angle, which lead to coupling in vibrational and magnetic properties of the material [7].

Though cubic $SrMnO_3$ based compounds have been studied in detail, such study on the hexagonal $Sr_{1-x}Ba_xMnO_3$ is not available. It should be noted here that hexagonal $SrMnO_3$ shows higher Neel temperature (T_N) (∼280 K) than the cubic structure (∼230 K) [5,7]. Therefore, if magnetic transition is coupled with its structural property, the spin-phonon coupling can be observed closer to room temperature. Hexagonal $SrMnO_3$ follows $P6_3/mmc$ symmetry [8]. In this symmetry, Mn ions are caged in two oxygen octahedra, MnO_6 octahedra and Mn_2O_9 bioctahedra. Antiferromagnetic coupling is reported both within the Mn_2O_9 entities and between the Mn ions in the corner-sharing octahedral [9]. However, there is no report available in literature regarding the coupling between the lattice and spin degrees of freedom in hexagonal $SrMnO_3$ based compounds, which is a crucial parameter for understanding the structural and magnetic properties of the system as well as for various applications. In this manuscript, we have probed the magnetic properties of hexagonal $Sr_{0.6}Ba_{0.4}MnO_3$ (SBMO) and examined the correlation between the magnetic properties and vibrational structure. It is observed that SBMO reveals antiferromagnetic transition at temperature (T_{N1}) 325 K, which is followed by another antiferromagnetic transition at temperature (T_{N2}) 227 K. Both the transitions are found to be magnetic field dependent; with the application of field, T_{N1} shifts towards lower temperature value, whereas T_{N2} shifts towards higher temperature value. Across these transition temperature values, Mn displacement vibrational Raman mode E_{1g} position softens and deviates from the anharmonic behavior. Line width of the E_{1g} mode also shows anomalous behavior confirming the spin phonon coupling in the system.

2. Experimental details

Polycrystalline hexagonal $Sr_{0.6}Ba_{0.4}MnO_3$ (SBMO) was prepared using solid state reaction method. We mixed $SrCO_3$, $BaCO_3$, and MnO_2 powders in stoichiometric ratio and performed wet grinding for six hours. After that the mixture was calcined at 1350 °C for 12 h. After calcination, mixture was again grinded for 2 h followed by sintering at 1400 °C for 12 h. Purity of the sample is confirmed using X-ray diffraction measurements and Rietveld fitting. X-ray diffraction measurements were performed using table top D2 Pha-

ser Bruker X-ray diffractometer. Raman measurements were performed using a HR800 Jobin-Yvon spectrometer. He-Ne laser with a wavelength of 632.8 nm was used to record Raman spectra in the temperature range of 90 K to 450 K. Magnetization measurement was carried out using 7 Tesla SQUID VSM (Quantum Design, USA).

3. Results and discussion

In Fig 1(a), we show the XRD pattern of SBMO sample. Rietveld refinement and Le Bail fitting are performed using Full Prof software, which confirm the single phase nature of the prepared sample and that the pattern follows P6$_3$/mmc symmetry, as reported for hexagonal SrMnO$_3$ [8]. Hexagonal structure of SBMO can exist in various polymorphs such as hexagonal 2H (AB), 6H (ABCACB) or 4H (ABAC) [10]. It is observed that XRD pattern fits well only for 4H-SBMO (Goodness of fit is 1.66). Lattice parameters are obtained as $a = b = 5.537$ Å and $c = 9.149$ Å and volume is 242.974 Å^3. The observed lattice parameters and volume of SBMO are higher than those reported for hexagonal SrMnO$_3$ [9], as expected due to larger ionic radii of Ba^{2+} than Sr^{2+}. To further confirm the hexagonal symmetry of the sample, room temperature Raman measurement was performed (Fig 1(b)). For hexagonal P6$_3$/mmc symmetry, five Raman modes are expected (A$_{1g}$ + E$_{1g}$ + 3-E$_{2g}$) [8,11–13]. We also obtained 5 Raman active vibrational modes, which confirm the symmetry of the sample. By comparing our data with the previous reports, assignment of the modes was done as shown in Fig. 1(b). The two modes E$_{2g}$(2) and E$_{1g}$ occurring at lower wavenumber (240 cm^{-1} and 334 cm^{-1}) are associated with the manganese displacement. In the crystal structure of SBMO (shown in Fig. 2), Mn4+ ion is surrounded by two different oxygen environments leading to formation of MnO$_6$ octahedra and Mn$_2$O$_9$ bioctahedra stacked along c-axis. Oxygen in this sample occurs at two sites, represented as O and O1 in the Fig.2. However, only O contributes in Raman active modes. E$_{2g}$(3) mode is associated with the bending mode involving O. E$_{2g}$(4) and A$_{1g}$ represent asymmetric and symmetric octahedral stretching mode [12]. It is noted that the mode positions of SBMO are occurring at lower wavenumber as compared to hexagonal SrMnO$_3$. This is expected since barium ions possess larger ionic radii and are heavier than strontium ions, which will decrease the vibrational frequency.

Magnetization measurements were performed using SQUID-VSM in zero field cooled warming (ZFC), field cooled cooling, (FCC) and field cooled warming (FCW) cycles at magnetic field of 0.01 Tesla (T). Observed magnetization versus temperature (M-T) curves are shown in Fig. 3(a) and derivative of the FCW curve is
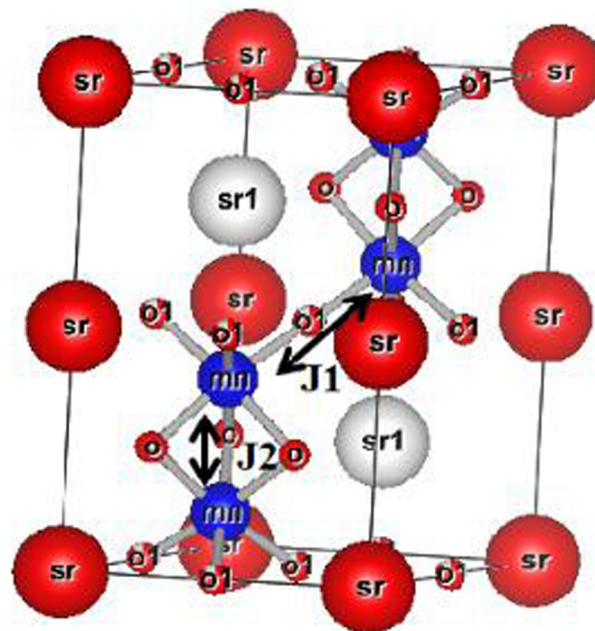

Fig. 2. Schematics of crystal structure of SBMO is plotted using Vesta software.

shown in Fig. 3(b). It is observed that magnetization decreases below 325 K with decrease in temperature, which is indicative of the antiferromagnetic nature of the transition and that Neel temperature (T$_N$) is 325 K. Further, a steep drop in magnetization is observed as the temperature is lowered below 227 K. Signature of this second transition is observed as maxima at 227 K in dM/dT versus temperature plot (Fig. 3(b)). From the M vs T curves and the derivative curve (dM/dT), therefore, we infer that the sample is undergoing two magnetic transitions, one at ∼ 227 K and other at ∼ 325 K. This behavior is observed in all the measurement cycles. There is no thermal hysteresis between FCC and FCW cycles, suggestive of second order nature of the magnetic transition. Upper Inset of Fig. 3(a) shows the M-T curve in FCW cycle measured at 7T, while its temperature derivative is shown in the Fig. 3(b) along with the derivative data obtained for FCW cycle measured at 0.01 T. It is observed that at 7 T the high temperature transition at 325 K (for 0.01 T) is shifted slightly towards lower temperature value of 320 K, whereas the magnetic transition at
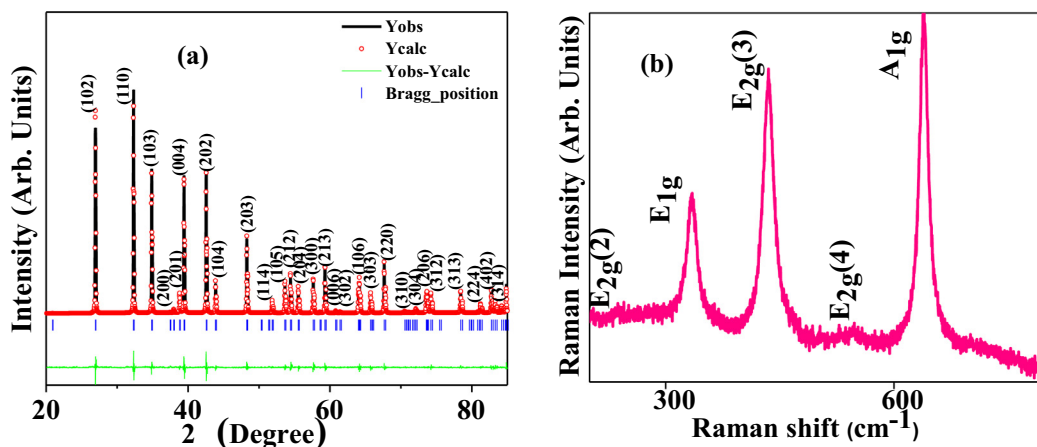

Fig. 1. (a) XRD pattern of SBMO with Rietveld and Le Bail fitting. (b) Room temperature Raman spectrum of SBMO.